Attenuation Relationships for Shallow Crustal Earthquakes Based on California Strong Motion Data

K. Sadigh
C.-Y. Chang
J.A. Egan
F. Makdisi
R.R. Youngs
Geomatrix Consultants

ABSTRACT

Attenuation relationships are presented for peak acceleration and response spectral accelerations from shallow crustal earthquakes. The relationships are based on strong motion data primarily from California earthquakes. Relationships are presented for strike-slip and reverse-faulting earthquakes, rock and deep firm soil deposits, earthquakes of moment magnitude M 4 to 8+, and distances up to 100 km.

INTRODUCTION

In this paper we summarize attenuation relationships we have developed from the analysis of strong motion data recorded primarily in California. These relationships have evolved through several iterations as new data have been gathered. The starting point is the set of attenuation relationships for peak acceleration and 5 percent damped spectral accelerations for rock and soil sites presented by Sadigh *et al.* (1986). Subsequently, Sadigh *et al.* (1989, 1993) developed an updated version of the rock site attenuation relationships that included analyses of strong motion data from the 1989 M 7 Loma Prieta, 1992 M 7.3 Landers, and M 6.4 Big Bear earthquakes. In this paper we present an updated version of the soil site attenuation relationships that also includes analysis of strong motion data from the 1994 M 6.7 Northridge earthquake, together with rock site attenuation models.

STRONG MOTION DATA

The ground motion data on which the attenuation relationships are based consist primarily of accelerograms from California earthquakes of moment magnitude M 3.8 and greater recorded at sites within 200 km of the rupture surface. Data from the Gazli, USSR (1976) and Tabas, Iran (1978) earthquakes were also included to provide more large magnitude data. Table 1 lists the earthquakes that have been considered in the development of these relationships. Figure 1 shows the distributions of these events in terms of magnitude and source to site distance. We characterize the earthquake size by moment magnitude, M, as defined by Hanks and Kanamori (1979). Distance is defined as the minimum distance to the rupture surface, r_{rup}. However, for many of the smaller magnitude events, rupture surfaces have not been defined and we use hypocentral distance. Because the dimensions of rupture for small events are usually much smaller than the distances to the recording stations, we do not believe that the use of hypocentral distance introduces significant bias into the attenuation models. We distinguish between strike-slip and reverse-faulting earthquakes by the rake angle of rupture, with rake angles greater than 45° considered reverse-faulting events, and rake angles less than 45° considered strike-slip events. Examination of the peak motion data from the small number of normal-faulting earthquakes in the data set indicated that they were not significantly different from peak motions from strike-slip earthquakes. Therefore, the normal and strike-slip earthquakes were combined into a single category. Peak horizontal acceleration (PGA) and response spectral acceleration (SA) are represented by the geometric mean of the two horizontal components.

Attenuation relationships are presented for two general site categories, rock and deep soil. Rock sites are those with bedrock within about a meter from the surface. Recent studies of the shear wave velocities at many strong motion stations that have been classified in the past as rock indicate that the surface velocity often falls below the classical rock definition of >750 m/sec, and there is usually a strong velocity gradient because of near-surface weathering and fracturing. Thus, the site conditions representative of the rock attenua-

TABLE 1
List of Earthquakes Used to Develop Attenuation Relationships

Earthquake	Date	M	Fault Type[1]	Distance Range (km)	No. of Records[2]	
					R	DS
Kern County,CA	1952/07/21	7.4	RV	120.5–224.0	0	3
Port Hueneme, CA	1957/03/18	4.7	RV	14.1–14.1	0	1
Daly City, CA	1957/03/22	5.3	RV	9.5–9.5	1	0
Parkfield, CA	1966/06/27	6.1	SS	0.1–230.0	1	6
Borrego Mtn., CA	1968/04/09	6.6	SS	113.0–261.0	5	3
Santa Rosa, CA (A)	1969/10/02	5.6	SS	80.0–113.0	1	2
Santa Rosa, CA (B)	1969/10/02	5.7	SS	78.9–112.0	1	2
Lytle Creek, CA	1970/09/12	5.3	RV	19.7–76.0	5	2
San Fernando, CA	1971/02/09	6.6	RV	2.8–305.0	11	14
Lake Isabella, CA	1971/03/08	4.1	SS	8.9–8.9	1	0
Bear Valley, CA	1972/02/24	4.7	SS	2.5–2.5	1	0
Point Mugu, CA	1973/02/21	5.6	RV	25.0–25.0	0	1
Hollister, CA	1974/11/28	5.2	SS	39.0–39.0	1	0
Oroville, CA	1975/08/01	5.9	SS	9.5–35.8	2	2
Oroville, CA (R)	1975/08/02	5.1	SS	12.7–14.6	0	2
Oroville, CA (S)	1975/08/02	5.2	SS	12.4–15.0	0	2
Oroville, CA (A)	1975/08/03	4.6	SS	8.4–14.9	1	6
Oroville, CA (B)	1975/08/03	4.1	SS	7.7–15.0	1	6
Oroville, CA (F)	1975/08/06	4.7	SS	10.9–16.1	1	7
Oroville, CA (K)	1975/08/08	4.9	SS	6.5–13.3	2	5
Oroville, CA (N)	1975/08/11	4.3	SS	2.5–11.6	2	4
Oroville, CA (P)	1975/08/16	4.0	SS	9.5–12.3	3	5
Oroville, CA (T)	1975/09/26	4.0	SS	10.8–19.9	3	5
Oroville, CA (U)	1975/09/27	4.6	SS	8.6–22.4	3	5
Gazli, USSR	1976/05/17	6.8	RV	3.0–3.0	1	0
Calipatria Swarm,CA	1976/11/04	4.9	SS	13.6–26.4	1	2
Santa Barbara, CA	1978/08/13	6.0	RV	18.5–21.0	2	1
Tabas, Iran	1978/09/16	7.4	RV	17.0–172.0	3	0
Coyote Lake, CA	1979/08/06	5.7	SS	3.1–63.3	4	7
Imperial Valley, CA	1979/10/15	6.5	SS	0.5–158.0	4	33
Imp.Val., CA (A02)	1979/10/15	3.8	SS	11.6–32.2	0	6
Imp.Val., CA (A03)	1979/10/15	5.2	SS	12.2–27.1	0	15
Imp.Val., CA (A05)	1979/10/15	4.0	SS	9.7–19.5	0	2
Imp.Val., CA (A07)	1979/10/15	4.2	SS	14.4–24.9	0	3
Imp.Val., CA (A10)	1979/10/15	4.2	SS	10.6–21.6	0	3
Imp.Val., CA (A13)	1979/10/15	4.6	SS	9.6–10.2	0	2
Imp.Val., CA (A15)	1979/10/15	4.3	SS	11.9–24.6	0	3
Imp.Val., CA (A16)	1979/10/15	4.0	SS	5.2–5.2	0	1
Imp.Val., CA (A21)	1979/10/15	4.5	SS	10.4–21.2	0	2
Imp.Val., CA (A22)	1979/10/15	4.5	RV	23.6–27.6	1	1
Imp.Val., CA (A25)	1979/10/15	5.1	RV	14.8–33.8	0	9
Imp.Val., CA (A26)	1979/10/15	4.0	SS	12.1–13.9	0	2
Imp.Val., CA (A27)	1979/10/15	4.1	SS	13.2–13.2	0	1

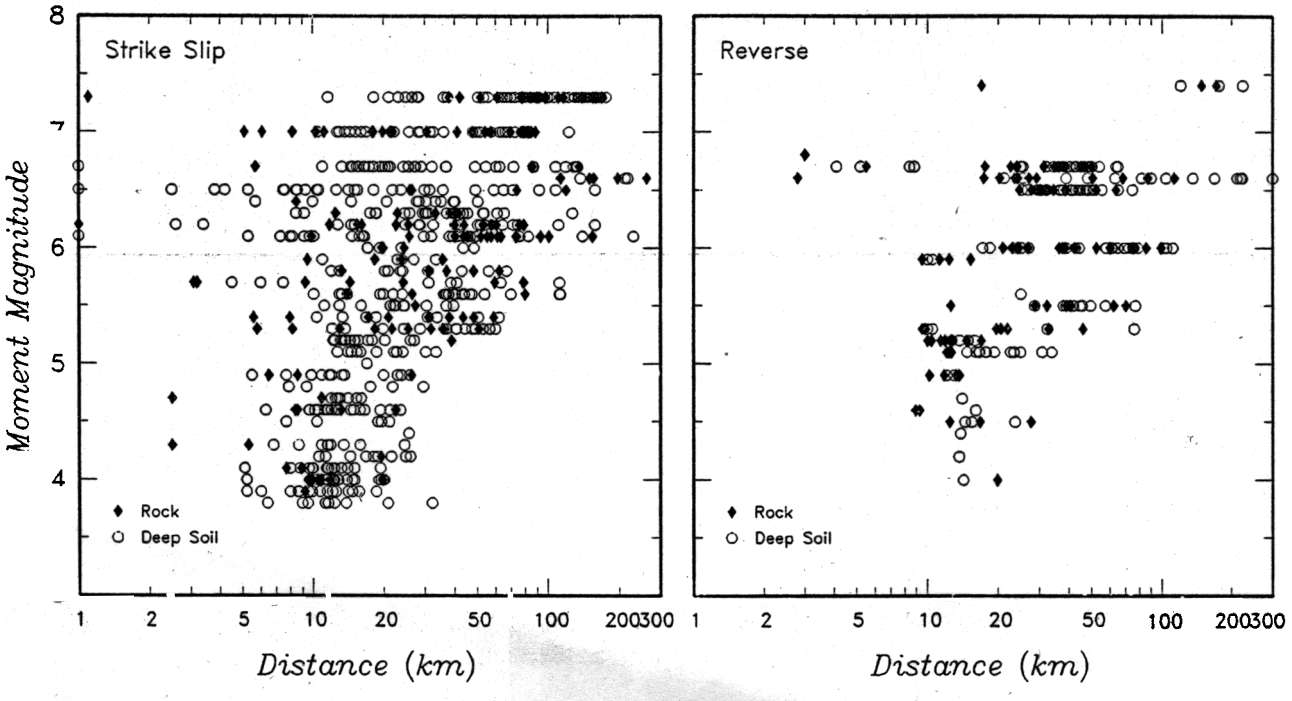

▲ **Figure 1.** Distribution of strong motion data used in development of attenuation relationships.

tion models given here should be considered soft rock. The deep soil data are from sites with greater than 20 m of soil over bedrock. We have not included data from very soft soil sites, such as those on San Francisco bay mud. Thus, the relationships are considered appropriate for deep, firm soil deposits. The data used in the analyses are from free-field recordings, that is from instruments housed in instrument shelters located near the ground surface and from the ground floor of small, light structures.

ATTENUATION MODEL DEVELOPMENT

Historically there are typically more data for peak acceleration than for response spectral acceleration, and the set of digitized and processed accelerograms tends to be the larger amplitude recordings from any individual earthquake. Therefore, the process that we have used to develop the attenuation relationships consists of two stages. First, attenuation relationships are developed for PGA by regression analyses using the general form

$$\ln(\mathrm{PGA}) = C_1 + C_2 M + C_3 \ln\left(r_{rup} + C_4 e^{C_5 M}\right) + C_6 Z_T \qquad (1)$$

where Z_T is an indicator variable taking the value 1 for reverse events and 0 for strike slip events. We have found the need to develop different coefficients for events larger and smaller than $M \approx 6\frac{1}{2}$ to account for near-field saturation effects.

In the second stage of the analysis, relationships for spectral amplification (SA/PGA) are fit to the response spectral ordinate data normalized by the PGA of the recordings. The form that we have found to work well is:

$$\ln(\mathrm{SA/PGA}) = C_7 + C_8(8.5 - M)^{2.5} + C_9 \ln\left(r_{rup} + C_4 e^{C_5 M}\right). \qquad (2)$$

In addition, Sadigh *et al.* (1993) added a term to account for near-field high-frequency motion (coefficient C_7 in Table 2).

The final attenuation models for SA are obtained by combining (1) and (2). The resulting parameters were then smoothed to produce attenuation relationships that predict smooth response spectra over the full range of magnitudes (M 4 to 8+) and distances (r_{rup} 0 to 100 km).

Once the median relationships were defined, the database was used to compute standard errors for PGA and SA at individual periods. The standard errors were found to be dependent on magnitude (Youngs *et al.*, 1995) and were represented by linear relationships between magnitude and standard error. The relationships for individual periods were smoothed to produce smooth estimates of 84th percentile response spectra.

The attenuation models that we have developed are listed in Tables 2 through 4 for rock and deep soil site conditions, respectively. Figures 2 and 3 show comparisons of the median attenuation relationships and recorded PGA data for strike slip and reverse earthquakes, respectively. Figure 4 shows the predicted median spectral shapes for rock and deep soil site motions.

TABLE 2

Attenuation Relationships of Horizontal Response Spectral Accelerations (5% Damping) for Rock Sites

$$\ln(y) = C_1 + C_2 M + C_3 (8.5 - M)^{2.5} + C_4 \ln\left(r_{rup} + \exp(C_5 + C_6 M)\right) + C_7 \ln\left(r_{rup} + 2\right)$$

Period(s)	C_1	C_2	C_3	C_4	C_5	C_6	C_7
			For M ≤ 6.5				
PGA	−0.624	1.0	0.000	−2.100	1.29649	0.250	0.0
0.07	0.110	1.0	0.006	−2.128	1.29649	0.250	−0.082
0.10	0.275	1.0	0.006	−2.148	1.29649	0.250	−0.041
0.20	0.153	1.0	−0.004	−2.080	1.29649	0.250	0.0
0.30	−0.057	1.0	−0.017	−2.028	1.29649	0.250	0.0
0.40	−0.298	1.0	−0.028	−1.990	1.29649	0.250	0.0
0.50	−0.588		−0.040	−1.945	1.29649	0.250	0.0
0.75	−1.208	.0	−0.050	−1.865	1.29649	0.250	0.0
1.00	−1.705	.0	−0.055	−1.800	1.29649	0.250	0.0
1.50	−2.407	.0	−0.065	−1.725	1.29649	0.250	0.0
2.00	−2.945	.0	−0.070	−1.670	1.29649	0.250	0.0
3.00	−3.700	.0	−0.080	−1.610	1.29649	0.250	0.0
4.00	−4.230	.0	−0.100	−1.570	1.29649	0.250	0.0
			For M > 6.5				
PGA	−1.274	1.1	0.000	−2.100	−0.48451	0.524	0.0
0.07	−0.540	1.1	0.006	−2.128	−0.48451	0.524	−0.082
0.10	−0.375	1.1	0.006	−2.148	−0.48451	0.524	−0.041
0.20	−0.497	1.1	−0.004	−2.080	−0.48451	0.524	0.0
0.30	−0.707	1.1	−0.017	−2.028	−0.48451	0.524	0.0
0.40	−0.948	1.1	−0.028	−1.990	−0.48451	0.524	0.0
0.50	−1.238	1.1	−0.040	−1.945	−0.48451	0.524	0.0
0.75	−1.858	1.1	−0.050	−1.865	−0.48451	0.524	0.0
1.00	−2.355	1.1	−0.055	−1.800	−0.48451	0.524	0.0
1.50	−3.057	1.1	−0.065	−1.725	−0.48451	0.524	0.0
2.00	−3.595	1.1	−0.070	−1.670	−0.48451	0.524	0.0
3.00	−4.350	1.1	−0.080	−1.610	−0.48451	0.524	0.0
4.00	−4.880	1.1	−0.100	−1.570	−0.48451	0.524	0.0

Note: Relationships for reverse/thrust faulting are obtained by multiplying the above strike-slip amplitudes by 1.2.

DISCUSSION

The attenuation relationships listed in Tables 2 through 4 are considered applicable for estimating free field ground motions from shallow crustal earthquakes in the magnitude range of M 4 to 8+. Shallow crustal earthquakes are those that occur on faults within the upper 20 to 25 km of continental crust. The relationships were developed for reverse and strike-slip faulting earthquakes. We did not find a significant difference between peak motions from strike-slip earthquakes and the limited number of data from normal faulting earthquakes and combined these two types of earthquakes into a single category. The data used to develop the relationships are primarily from California and occur in both compressional and extensional stress regimes. Campbell (1987) found no significant difference between the peak motions for events occurring in compressional and extensional stress regimes.

The attenuation relationships show an expected trend for soil versus rock motions, *i.e.*, soil amplitudes are larger than rock where the rock motions are low because of site amplification in the lower velocity soil layers. Where the rock motions are high, the soil motions become lower than rock motions presumably because of nonlinear site response effects. The rock motion spectral shapes change with distance. However, no significant effect of distance was observed in the soil spectral shapes within 50 km of the rup-

TABLE 3
Dispersion Relationships for Horizontal Rock Motion

Period	Sigma [ln(y)]
	1.39 – 0.14M; 0.38 for $M \geq$ 7.21
	1.40 – 0.14M; 0.39 for $M \geq$ 7.21
	1.41 – 0.14M; 0.40 for $M \geq$ 7.21
	1.43 – 0.14M; 0.42 for $M \geq$ 7.21
	1.45 – 0.14M; 0.44 for $M \geq$ 7.21
	1.48 – 0.14M; 0.47 for $M \geq$ 7.21
	1.50 – 0.14M; 0.49 for $M \geq$ 7.21
	1.52 – 0.14M; 0.51 for $M \geq$ 7.21
	1.53 – 0.14M; 0.52 for $M \geq$ 7.21
	1.53 – 0.14M; 0.52 for $M \geq$ 7.21

TABLE 4
Attenuation Relationship Coefficients for Deep Soil Sites

$$\ln(y) = C_1 + C_2 M - C_3 \ln\left(r_{rup} + C_4 e^{C_5 M}\right) + C_6 + C_7 (8.5 - M)^{2.5}$$

where y is spectral accleration in g
C_1 = –2.17 for strike-slip, –1.92 for reverse and thrust earthquakes
C_2 = 1.0
C_3 = 1.70
C_4 = 2.1863, C_5 = 0.32 for $M \leq 6.5$
C_4 = 0.3825, C_5 = 0.5882 for $M > 6.5$
r_{rup} = closest distance to rupture surface

Period (sec)	C_6 Strike-Slip	C_6 Reverse	C_7	Standard Error[1]
	0.0	0.0	0.(	1.52 – 0.16M
	0.4572	0.4572	0.(	1.54 – 0.16M
	0.6395	0.6395	0.(	1.54 – 0.16M
	0.9187	0.9187	–0.(	1.565– 0.16M
	0.9547	0.9547	–0.(	1.58 – 0.16M
	0.9251	0.9005	–0.(	1.595 – 0.16M
	0.8494	0.8285	–0.(	1.61 – 0.16M
	0.7010	0.6802	–0.(	1.635 – 0.16M
	0.5665	0.5075	–0.(	1.66 – 0.16M
	0.3235	0.2215	–0.(	1.69 – 0.16M
	0.1001	–0.0526	–0.·	1.70 – 0.16M
	–0.2801	–0.4905	–0.·	1.71 – 0.16M
	–0.6274	–0.8907	–0.·	1.71 – 0.16M

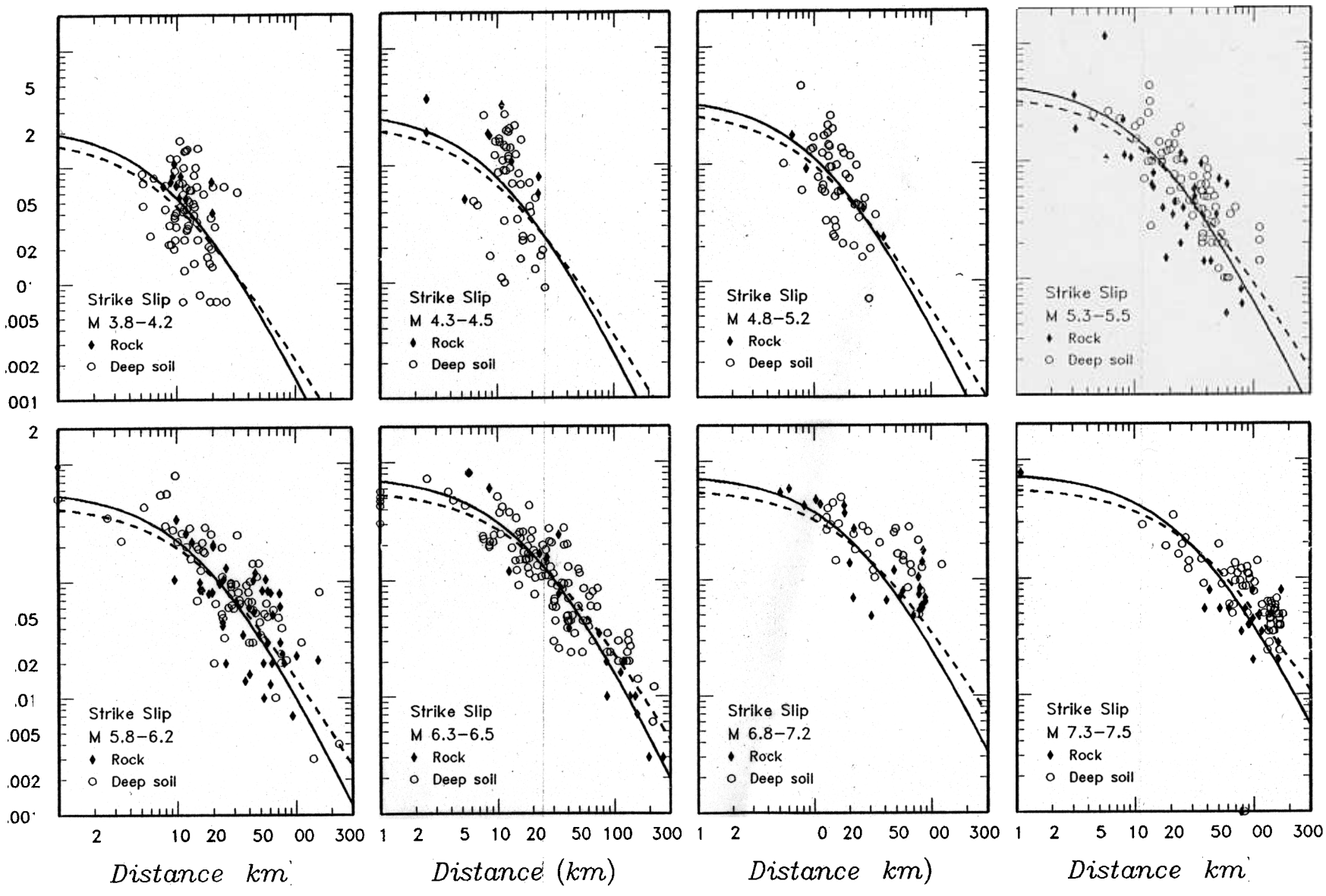

Figure 2. Comparison of PGA data for strike-slip (rake < 45°) earthquakes with median attenuation relationships listed in Tables 2 through 4. Solid line is the rock motion relationship from Table 2 and dashed line is the deep soil relationship from Table 4.

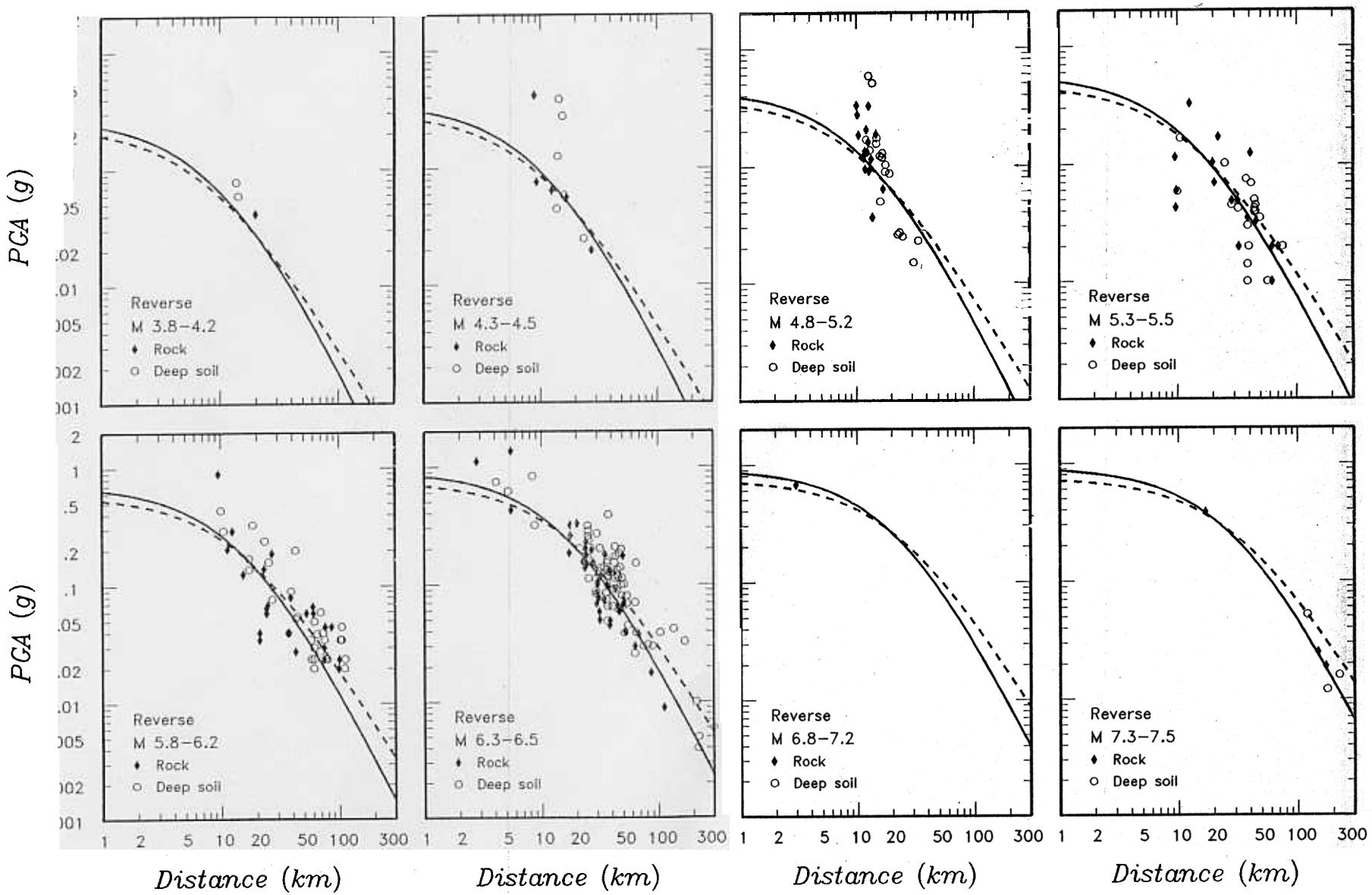

▲ **Figure 3.** Comparison of PGA data for reverse (rake > 45°) earthquakes with median attenuation relationships listed in Tables 2 through 4. Solid line is the rock motion relationship from Table 2 and dashed line is the deep soil relationship from Table 4.

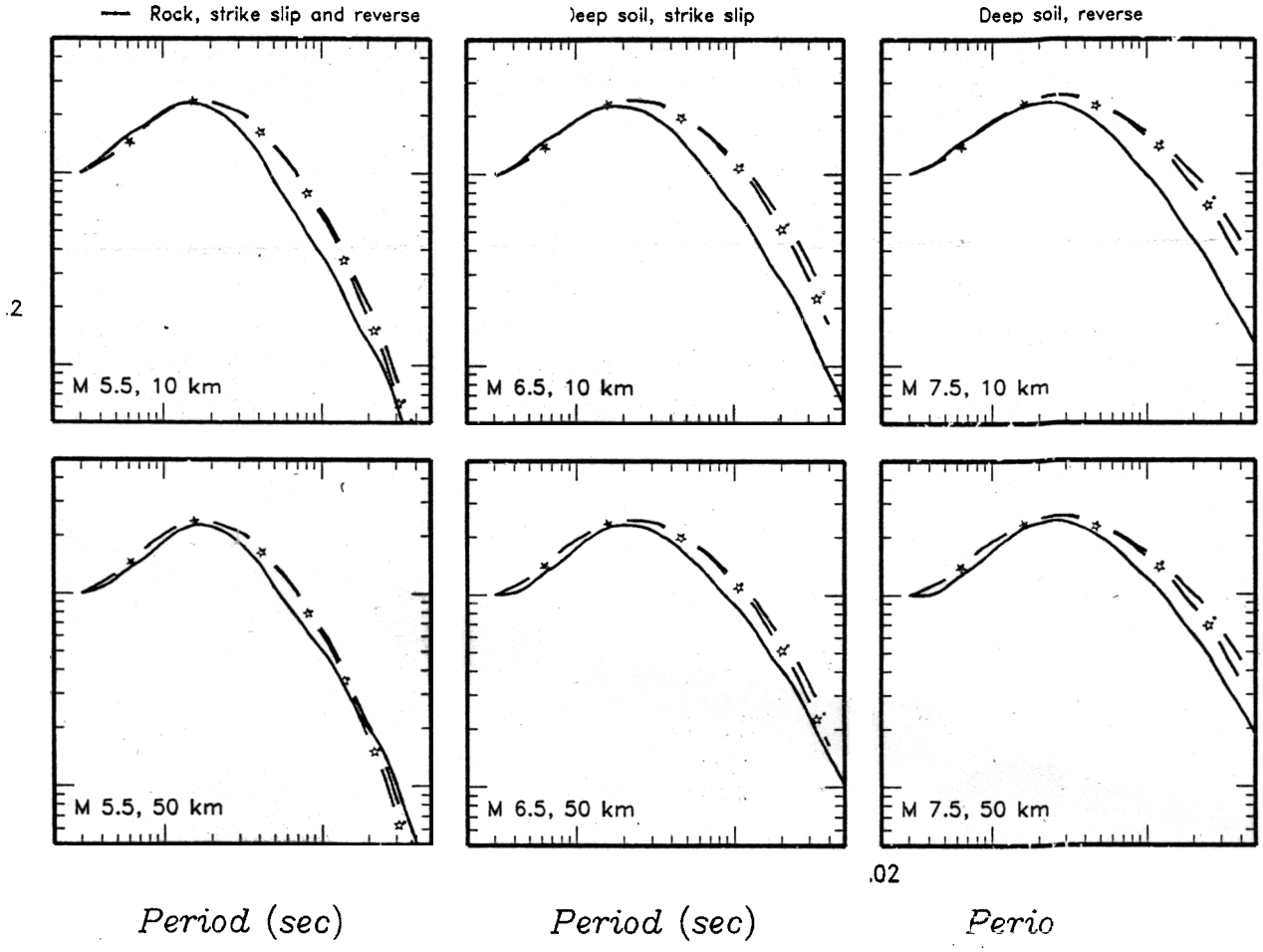

Figure 4. Comparison of spectral shapes (SA/PGA) obtained using the median attenuation relationships listed able through 4

ture. Sadigh *et al.* (1993) indicate that within 10 km of the rupture surface there are systematic differences between the fault-normal and fault-parallel components of long-period ground motion. Specifically, they recommend that the fault-normal component be increased by 20 percent over the geometric average values for spectral periods of 2.0 seconds and greater and the fault-parallel component would be expected to be 20 percent lower than the geometric average value.

REFERENCES

pbell, K.W. (1987). Predicting strong ground motion in Utah, in *Assessment of Regional Earthquake Hazards and Risk Along the Wasatch Front, Utah*, U.S. Geological Survey Open-File Report 87-585, **II**, L-1-120.

Hanks, T.C., and H. Kanamori (1979). A moment magnitude scale, *J. Geophys. Res.*, **84**, 2,348–2,350.

gh, K., C.-Y. Chang, N.A. Abrahamson, S.J. C iiou and M.: Power (1993). Specification of long-period gi ound motion updated attenuation relationships for rock site conditions an adjustment factors for near-fault effects, in *Proc. ATC-17-1 Seminar on Seismic Isolation, Passive Energy Dissipation, and Active Control*, March 11–12, San Francisco, California, 59–70.

adigh, K., C.-Y. Chang, F. Makdisi and J.A. Egan, (1989). Attenuation relationships for horizontal peak ground acceleration anc response spectral acceleration for rock sites (abs.), *Seism. Res. Lett.*, **60**, 19.

digh, K., J.A. Egan, and R.R. Youngs (1986). Specification of groun motion for seismic design of long period structures (abs.), *Earthquake Notes*, **57**, n. 1, 13. Relationships printed in W.B. Joyne and D.M. Boore (1988), Measurement, characterization, and prediction of strong ground motion, in *Earthquake Engineering an Soil Dynamics II—Recent Advances in Ground Motion Evaluatior* ASCE Geotechnical Special Publication 20, 43-102.

oungs, R.R., N.A. Abrahamson, F. Makdisi, and K. Sadigh (1995) Magnitude dependent dispersion in peak ground acceleratior *Bull. Seism. Soc. Am.*, **85**, 1,161–1,176.

Geomatrix Consultants
100 Pine St., 10th Floor
San Francisco, CA 94111